

# Numerical study of the transverse diffusion coefficient for a one component model of plasma

Cite as: Chaos **32**, 033103 (2022); <https://doi.org/10.1063/5.0068674>

Submitted: 26 August 2021 • Accepted: 08 February 2022 • Published Online: 03 March 2022

 Lorenzo Valvo and  Andrea Carati



View Online



Export Citation



CrossMark

## ARTICLES YOU MAY BE INTERESTED IN

### [A classical analog of the quantum Zeeman effect](#)

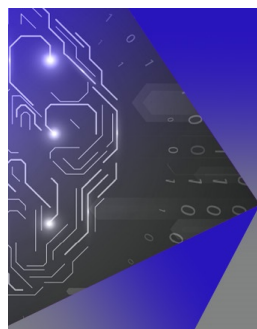
Chaos: An Interdisciplinary Journal of Nonlinear Science **32**, 033101 (2022); <https://doi.org/10.1063/5.0081254>

### [Understanding the origins of the basic equations of statistical fibrillatory dynamics](#)

Chaos: An Interdisciplinary Journal of Nonlinear Science **32**, 032101 (2022); <https://doi.org/10.1063/5.0062095>

### [Influence of time-delayed feedback on the dynamics of temporal localized structures in passively mode-locked semiconductor lasers](#)

Chaos: An Interdisciplinary Journal of Nonlinear Science **32**, 033102 (2022); <https://doi.org/10.1063/5.0075449>



## APL Machine Learning

Machine Learning for Applied Physics  
Applied Physics for Machine Learning

Now Open for Submissions

# Numerical study of the transverse diffusion coefficient for a one component model of plasma

Cite as: Chaos 32, 033103 (2022); doi: 10.1063/5.0068674

Submitted: 26 August 2021 · Accepted: 8 February 2022 ·

Published Online: 3 March 2022



View Online



Export Citation



CrossMark

Lorenzo Valvo<sup>a)</sup>  and Andrea Carati<sup>b)</sup> 

## AFFILIATIONS

Department of Mathematics, Università degli Studi di Milano, Via Saldini 50, 20133 Milano, Italy

<sup>a)</sup> Electronic mail: [lorenzovalvo@gmx.com](mailto:lorenzovalvo@gmx.com)

<sup>b)</sup> Author to whom correspondence should be addressed: [carati@mat.unimi.it](mailto:carati@mat.unimi.it)

## ABSTRACT

In this paper, we discuss the results of some molecular dynamics simulations of a magnetized one component plasma, targeted to estimate the diffusion coefficient  $D_{\perp}$  in the plane orthogonal to the magnetic field lines. We find that there exists a threshold with respect to the magnetic field strength  $|\vec{B}|$ : for weak magnetic field, the diffusion coefficients scale as  $1/|\vec{B}|^2$ , while a slower decay appears at high field strength. The relation of this transition with the different mixing properties of the microscopic dynamics is investigated by looking at the behavior of the velocity autocorrelation.

Published under an exclusive license by AIP Publishing. <https://doi.org/10.1063/5.0068674>

The diffusion process is well understood for stochastic motions,<sup>1</sup> which are supposed to mimic the behavior of a chaotic dynamical system. Many questions are instead left open in the study of the diffusive properties of a system, which is in a partially ordered state.<sup>2</sup> A central issue, as regards magnetized plasma confinement, is the diffusion of charged particles in the direction perpendicular to the magnetic field lines. A widely accepted law, predicting that the transversal diffusion  $D_{\perp}$  coefficient is proportional to the inverse of the square of the magnetic field strength  $|\vec{B}|$ , was proposed more than 50 years ago.<sup>3</sup> Being based on kinetic theory, this law is expected to hold whenever the microscopic dynamics is chaotic. However, as the magnetic field  $|\vec{B}|$  is increased, a partially ordered state seems to set in Refs. 4 and 5, at least for a pure electron plasma. Our purpose was to investigate the consequences (if any) of this transition on the diffusion process. Therefore, we have performed molecular dynamics simulations of a magnetized one component plasma, that is, a set of mutually interacting electrons subject to a constant external magnetic field. We estimate the diffusion coefficient  $D_{\perp}$  in the plane orthogonal to the field for different values of the magnetic field strength  $|\vec{B}|$ . We find that the kinetic law holds for low  $|\vec{B}|$  when the microscopic dynamics is chaotic. However, as the magnetic field grows, the diffusion coefficient seems to saturate to a plateau, while the microscopic state turns to a partially ordered one.

## I. INTRODUCTION

In the 1960s, there was a great exchange among research groups of plasma physics and of dynamical systems, as both were interested in the study of the  $1\frac{1}{2}$  Hamiltonian system that can represent the magnetic field lines; see Ref. 6 for a broad historical overview. In more recent years, another point of connection has become the study of diffusion process in the phase space; see Ref. 1. It has been shown that if the dynamics is not fully chaotic, then the process of diffusion in the phase space can be “not normal”; i.e., the mean square displacement does not necessarily grow linearly in time: the process is called super diffusive if the growth is faster than linear or subdiffusive otherwise; for a review, see Ref. 2. In both cases, there is no widespread agreement of the correct definition of the diffusion coefficient to be adopted.

Now, as it will be shown below, the equations of motion for a single electron in a one component plasma subject to an external constant magnetic field  $\vec{B}$  can be recasted in a dimensionless form, in which the only parameter appearing is the ratio  $\beta = \sqrt{4\pi}\omega_c/\omega_p$  among the cyclotron frequency  $\omega_c = eB/mc$  and the plasma frequency  $\omega_p = \sqrt{4\pi ne^2/m}$  (in the CGS system); here,  $n$  is the particle density and  $e$  the electronic charge. The parameter  $\beta$  measures the relative strength of the magnetic Lorentz force acting on a single electron, with respect to the electrostatic force due to all other electrons. In the limit of  $\beta \rightarrow +\infty$ , the equations of motions decouple

and the system reduces (formally) to a set of independent electrons in a constant magnetic field, i.e., to an integrable system.

Therefore, it can be conjectured that for high magnetic field strength, the dynamics will not be fully chaotic (see Refs. 4 and 5) and that the diffusion process in phase space may be “anomalous.” Actually, it is impossible for us to study numerically such process, and we limit ourselves to study the diffusion of the electrons in the physical space. To this end, we study the diffusion coefficient, defined as usual by<sup>8</sup>

$$D_{\perp} = \lim_{t \rightarrow \infty} \frac{\langle |\Delta \vec{x}_{\perp}|^2 \rangle}{4t}, \quad (1)$$

where  $|\Delta \vec{x}_{\perp}|^2$  is the mean displacement in the plane perpendicular to the magnetic field of the electrons from their initial positions and  $\langle \cdot \rangle$  is the phase average. On the contrary, in this paper, following a common attitude, averages will always be taken as time averages along the orbits. We have not investigated the relations between the two averages.

As regards physical applications, small values of  $D_{\perp}$  are important for the purpose of plasma confinement in fusion devices. This is another reason to investigate in which regime the diffusion coefficient is small.

Another dimensionless parameter that characterizes the state of a plasma is the coupling parameter  $\Gamma = e^2/(ak_B T)$ , where  $a$  is the interparticle spacing (related to the particle density  $n$  by the relation  $a = n^{-1/3}$ ),  $T$  the plasma temperature, and  $k_B$  as usual the Boltzmann constant. So defined,  $\Gamma$  is the ratio among the mean coulomb energy of a couple of nearest particles and the mean kinetic energy. The weak coupling regime is then defined by  $\Gamma < 1$  and the strong coupling regime by  $\Gamma \geq 1$ . Up to now, because of the reasons explained in the following, molecular dynamics (MD) simulations have been performed mainly in the strongly coupled case, while the weakly coupled regime has been addressed mostly by kinetic theory.

In the literature, it is possible to find different estimates for the diffusion coefficient. The oldest one,<sup>9</sup> predicting the scaling law  $D_{\perp} \propto \beta^{-2}$ , is obtained in the frame of the kinetic theory in the weak coupling regime. However, other different theories have been proposed in the years, each giving a different law for the dependence of the diffusion coefficient  $D_{\perp}$  on the parameter  $\beta$ . A few of them are summarized in Table 1, p. 135003-2, of Ref. 9; another one is percolation theory (see Refs. 7, 10, and 11), which predicts scaling, such as  $\beta^{-0.7}$ . This law is in the closest agreement with our results. It was brought to our attention by an anonymous referee that we warmly thank.

However, none of the proposed theories is based on the loss of chaoticity in the Newtonian microscopic dynamics. Also, the numerical works found in the literature fail to address this point. In fact, up to now, the behavior of the diffusion coefficient has been investigated by MD mostly in the unmagnetized case; see, for instance, Refs. 12–14. The magnetized case was studied in Ref. 9 but only in the strong coupling regime: at the smallest value  $\Gamma = 1$ , a transition at  $\beta \approx 1$  in the behavior of  $D_{\perp}$  was observed, but the origin of such a transition was not discussed. A similar transition was observed also in two more recent works,<sup>15,16</sup> where the diffusion coefficient was studied numerically for  $\Gamma$  down to 0.1. However, those works were based on a so-called particle–particle

particle–mesh ( $P^3M$ ) code, which is a sort of hybrid between a kinetic and a MD code. We think that such a method is not suited to study the chaoticity of the microscopic dynamics. More on the connections between our results and the cited paper will be discussed in Sec. IV.

Therefore, in this paper, we perform a full MD simulation for different values of  $\beta$  for a system of  $N = 4096$  electrons, for a fixed value of  $\Gamma = 0.1$ , which is the smallest value we were able to manage. The aim is to verify for what value of  $\beta$  the transition in the behavior of  $D_{\perp}$  occurs and to observe the chaoticity of the dynamics by computing the time autocorrelation of the transverse particle velocity.

In Sec. II, we describe the model and the numeric algorithm used, in Sec. III, the numerical results are reported, while in Sec. IV, the conclusions follow.

## II. THE MODEL AND THE NUMERICAL SCHEME

The system we are considering is called in the literature a one component plasma, and it consists of a number  $N$  of electrons in a cubic box of side  $L$  with periodic boundary conditions, the electrons being subject to mutual Coulomb interactions, and to an external constant magnetic field  $\vec{B} = B\vec{e}_z$  ( $\vec{e}_z$  is the unit vector directed along the  $z$  axis). The density is then defined by  $n = N/L^3$ . This is considered a model of plasma as the positive ions are supposed to constitute a uniform neutralizing background.

If  $t$  denotes time and  $\vec{x}_i$  the position of the  $i$ th electron (with  $i = 1, \dots, N$ ), we define dimensionless variables

$$\vec{y}_i = a^{-1}\vec{x}_i, \quad \tau = \omega_c t \quad (2)$$

by rescaling distances with the interparticle spacing  $a = n^{-1/3}$  and time with the cyclotron frequency  $\omega_c$ . Using such variables, the equations of motion for the  $i$ th electron read

$$\frac{d^2 \vec{y}_i}{d\tau^2} = \vec{e}_z \times \frac{d\vec{y}_i}{d\tau} + \frac{1}{\beta^2} \vec{E}(\vec{y}_i), \quad (3)$$

where  $\vec{E}(\vec{y}_i)$  is the electric field acting on the  $i$ th electron due to all other charges. The electric field of a periodic system of charges can be computed via the Ewald formula (see, for example, Ref. 17)

$$\begin{aligned} \vec{E}(\vec{y}_i) = & \sum_{\vec{l}} \sum_{j=1}^N \frac{\vec{y}_{ij\vec{l}}}{|\vec{y}_{ij\vec{l}}|^3} \left[ \operatorname{erfc}(\alpha|\vec{y}_{ij\vec{l}}|) + \frac{2\alpha|\vec{y}_{ij\vec{l}}|}{\sqrt{\pi}} \exp(-\alpha^2|\vec{y}_{ij\vec{l}}|^2) \right] \\ & + \frac{4\pi}{N} \sum_{\vec{q} \neq 0} \sum_{j=1}^N \frac{\vec{q}}{q^2} e^{-q^2/4\alpha^2} \sin(\vec{q} \cdot \vec{y}_{ij}), \quad \alpha = \sqrt{\pi} N^{-1/6}, \quad (4) \end{aligned}$$

where  $\vec{l}$  is a triplet of integers denoting the position of an image cell, while  $\vec{q}$  is a vector in the reciprocal lattice, i.e., defined by  $\vec{q} = 2\pi\vec{n}/L$  with  $\vec{n}$  being an integer vector, and finally, we have defined  $\vec{y}_{ij\vec{l}} = \vec{y}_i - \vec{y}_j + \vec{l}\sqrt[3]{N}$ . The two series are truncated as to keep the relative error below  $10^{-7}$ , which is smaller than the relative error of the energy conservation in a single numerical step.

Of the two dimensionless parameters of the problem, only  $\beta$  appears in the equations of motion. The parameter  $\Gamma$  enters through the choice of the initial data: in fact, while the positions are extracted from a uniform distribution, the velocities are taken from a Maxwell

distribution, and the temperature is uniquely determined by  $\Gamma$ . With this choice, at the beginning of each simulation, the system is out of equilibrium: therefore, there is a drift of the kinetic energy, and the system reaches a different, random, temperature. In order to fix the temperature to the desired value, we operate in this way: after extracting the initial values, we let the system evolve until equilibrium is reached, i.e., until the kinetic energy appears to stabilize. We then generate new velocities again with a Maxwell distribution at temperature  $T$  and repeat the process until the kinetic energy appears to be constant and close to the chosen value.

Equation (3) was integrated using a symplectic splitting algorithm.<sup>18</sup> The total Hamiltonian

$$H = \frac{1}{2} \sum_k \left( \vec{p}_k + \frac{1}{2} \vec{e}_z \times \vec{y}_k \right)^2 + \frac{1}{\beta^2} V(\vec{y}_1, \dots, \vec{y}_N), \quad (5)$$

where  $V(\vec{y}_1, \dots, \vec{y}_N)$  is the Coulomb potential of the electrons computed according to the Ewald prescription and was split as  $H = H_1 + H_2$ , where

$$H_1 \stackrel{\text{def}}{=} \frac{1}{2} \sum_k \left( \vec{p}_k + \frac{1}{2} \vec{e}_z \times \vec{y}_k \right)^2, \quad H_2 \stackrel{\text{def}}{=} V(\vec{y}_1, \dots, \vec{y}_N). \quad (6)$$

Now, denoting by  $\Phi_1^t$  the flow determined in the phase space by the Hamiltonian  $H_1$  and by  $\Phi_2^t$  the one due to the Hamiltonian  $H_2$ , the integration algorithm is obtained simply by composition  $\Phi \stackrel{\text{def}}{=} \Phi_1^{\delta t/2} \circ \Phi_2^{\delta t} \circ \Phi_1^{\delta t/2}$ , where  $\delta t$  is the time step. Such a time step was chosen so that the energy conservation was better than a part over  $10^4$  in all the simulations. In particular, we choose  $\delta t = 2\pi C(\beta) 10^{-4}$ , where the factor  $C(\beta)$  is taken to be equal to  $\beta$  for  $\beta < 1$  and to be equal to 1 for larger  $\beta$ . In Fig. 1, we report the relative error of the energy conservation as a function of the number of integration step for a typical run. The number of steps used was  $4 \times 10^6$  for  $\beta \leq 2.5$ , four times this number for  $\beta$  larger.

In MD simulations, the choice of the number  $N$  of particles is always an issue, all the more in the context of a weakly coupled plasma. For a very rough estimation, we made the following considerations: the fundamental cell of the simulation should have a side larger than the Debye length  $\lambda_D$ , which in our units reads  $\lambda_D = \sqrt{1/\Gamma}$ . The first of (2) implies that  $L = N^{1/3}$  so that the requirement  $L > \lambda_D$  in our units becomes  $N > \Gamma^{-3/2}$ . As the Coulomb force is long range, the computational cost scales as a power of  $N$ . With a clever use of the Ewald summation formula, see Ref. 19, the computational cost scales (asymptotically) as<sup>20</sup>  $N^{3/2}$ . Therefore, we cannot afford to choose a value much bigger than  $N = 4096$ . In any case, for  $\Gamma = 0.1$ , our constraint reads  $N > 32$ , and therefore, with our choice of  $N = 4096$ , we have  $L \simeq 5\lambda_D$ .

Another interesting length scale that appears in the problem is the Larmor radius  $r_l$ , i.e., the gyration radius of the electrons determined by the magnetic Lorentz force due to the external magnetic field  $B$ . A simple computation shows that one has  $r_l/L = \sqrt{2/\Gamma}/\beta N^{1/3}$ . For the smallest value of  $\beta$  used in our computations, i.e.,  $\beta = 0.25$ , the Larmor radius is slightly larger than the side of the simulation cell because one gets  $r_l \simeq 1.1L$ . On the contrary,  $r_l$  turns out to be well below the Debye length for the largest value of  $\beta = 10$ .

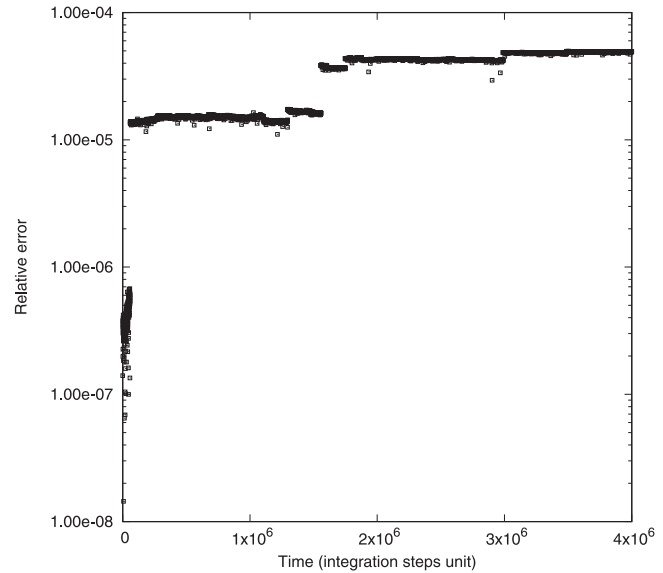


FIG. 1. Relative error of the energy conservation as a function of the number of integration steps. Data refer to a case with  $\beta = 1$  and  $N = 4096$  particles.

### III. RESULTS

We recall that the transverse diffusion coefficient is defined by (1), where

$$|\Delta \vec{x}_\perp|^2 \stackrel{\text{def}}{=} \frac{\sum_k (|x_k(t) - x_k(t_0)|^2 + |y_k(t) - y_k(t_0)|^2)}{N} \quad (7)$$

is the mean particle displacement in the plane orthogonal to the magnetic field  $\vec{B}$  (we recall that the latter was taken to be directed at the  $z$  axis) and the parentheses denote the time average along the orbit. To estimate this quantity, we proceed as follows.

Let  $\delta t$  be the integration step and  $M_{tot}$  the total number of integration steps. Let  $j$  be also an integer smaller than a fixed fraction  $M'$  of  $M_{tot}$  (we take one sixteenth), and then the time averages of  $\langle |\Delta \vec{x}_\perp|^2 \rangle$  at time  $t_j = j\delta t$  were computed as

$$\begin{aligned} & \langle |\Delta \vec{x}_\perp|^2 \rangle (t_j) \\ &= \frac{1}{M} \sum_{h=1}^M \left( \frac{1}{N} \sum_{k=1}^N (|x_k(t_{h+j}) - x_k(t_h)|^2 + |y_k(t_{h+j}) - y_k(t_h)|^2) \right), \end{aligned} \quad (8)$$

where  $M = M_{tot} - M'$ . After plotting  $\langle |\Delta \vec{x}_\perp|^2 \rangle$  as a function of time, we fit the tail with a straight line whose angular coefficient (divided by four) is an estimate of the diffusion coefficient. The values computed in such way can be found in Table I (second entry).

The whole set of our plots (in a log-log scale) can be found in Fig. 2; as usual, they display diffusive (linear) behavior only after a certain time (the so-called ballistic jump). Therefore, we also restricted the sets of points to the latter time window to exclude small times.

**TABLE I.** Values of the diffusion coefficient  $D_{\perp}$ , together with the values of the parameter  $A$ ,  $\omega$ , and  $\gamma$  that appear in the fit of velocity autocorrelation.

$\beta$	$D_{\perp}$	$D_{\perp}^a$	$A$	$\omega$	$\gamma$
0.25	18.1	17.9	9.90	0.253	0.169
0.50	5.61	5.91	9.85	0.506	0.169
0.75	2.68	2.83	9.80	0.754	0.167
1.00	1.56	1.63	10.1	1.01	0.164
1.25	1.03	1.07	9.95	1.258	0.166
2.00	0.428	0.434	9.90	2.022	0.165
2.50	0.327	0.342	9.75	2.518	0.171
4.00	0.212	0.200	10.0	4.046	0.168
5.00	0.188	0.184	10.35	5.035	0.164
10.0	0.133	0.146	10.30	10.06	0.157

<sup>a</sup>Computed from the velocity correlation by formula (9).

The results of our computations are summarized in Fig. 3. There, in a logarithmic scale, the numerically computed values of the coefficient  $D_{\perp}$  are reported (full circles) as a function of  $\beta$ . All the simulations were performed at the same value of  $\Gamma = 0.1$ . The solid line is the plot of the function  $D_{\perp} = \frac{\gamma A}{\gamma^2 + \beta^2}$ , with  $\gamma = 0.168$  and  $A = 9.9$ . It can be checked that this function agrees very well with the numerical results for  $\beta < 2$ . We remark that, for small values of  $\gamma$ , this function decreases as  $\beta^{-2}$ ; i.e., for  $\beta < 2$ , the computed values of  $D_{\perp}$  agree with the prediction of the kinetic theory. However, by further increasing the magnetic field above a value about 2, the plot shows a “knee”: the diffusion coefficient appears to obey a different

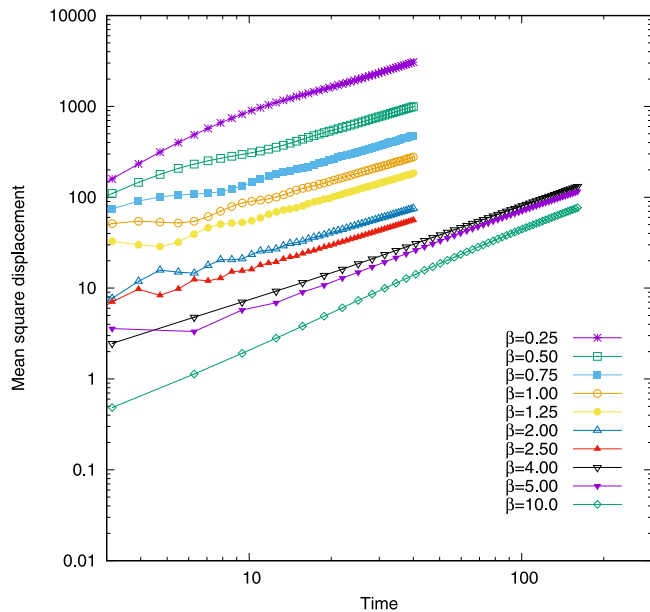


**FIG. 2.** The average square displacement as a function of time. It is interesting to observe the initial nondiffusive behavior, which becomes more evident as  $\beta$  is increased.

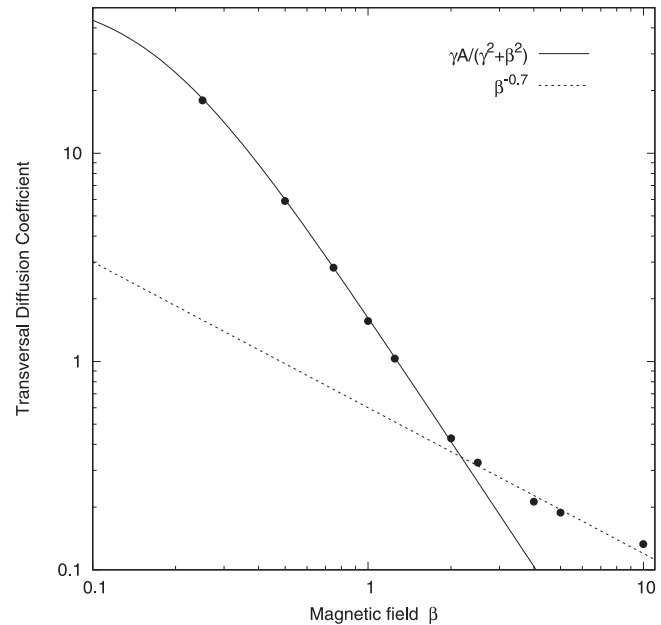


**FIG. 3.** Diffusion coefficient  $D_{\perp}$  perpendicular to the magnetic field vs  $\beta$  computed by MD simulations. Circles are the numerical results, while the solid line is the plot of the function  $D_{\perp} = \frac{\gamma A}{\gamma^2 + \beta^2}$ , with  $\gamma = 0.168$  and  $A = 9.9$ . Such values are obtained from the autocorrelation of the electron velocities, as explained in the text. The broken line is the plot of the function  $D_{\perp} \simeq \beta^{-0.7}$ , corresponding to the law found in Ref. 7.

law. These results are in agreement with Fig. 5(a) of Ref. 16. Notice that for such a value of  $\beta$ , the Larmor radius  $r_l$  is slightly smaller than Debye length.

The law  $D_{\perp} = \frac{\gamma A}{\gamma^2 + \beta^2}$  was not obtained by interpolation, but by the use of the following argument. Let us introduce the velocity autocorrelation  $\langle \vec{v}_{\perp}(t) \cdot \vec{v}_{\perp}(0) \rangle$ , where  $\vec{v}_{\perp}$  is the component of the mean particle velocity transverse to the magnetic field, and the brackets denote the time averages along the orbit. Then, the diffusion coefficient can be expressed<sup>21</sup> as

$$D_{\perp} = \frac{1}{2} \int_0^{+\infty} \langle \vec{v}_{\perp}(t) \cdot \vec{v}_{\perp}(0) \rangle dt \tag{9}$$

whenever the velocity autocorrelation decays at  $t \rightarrow +\infty$  fast enough. Let us introduce a function  $f(t)$  to describe this decay by setting

$$\langle \vec{v}_{\perp}(t) \cdot \vec{v}_{\perp}(0) \rangle \simeq \langle \vec{v}_{\perp}(0) \cdot \vec{v}_{\perp}(0) \rangle \cos(\omega_c t) f(t). \tag{10}$$

Recalling the electronic dynamics, we expect that due to the gyration along the magnetic field lines alone,  $\langle \vec{v}_{\perp}(t) \cdot \vec{v}_{\perp}(0) \rangle$  would oscillate with the cyclotron frequency  $\omega_c$ . However, the electric interaction between the electrons instead determines a loss of coherence of the electronic motion and thus the decaying to zero of the autocorrelation. A common choice is to consider an exponential

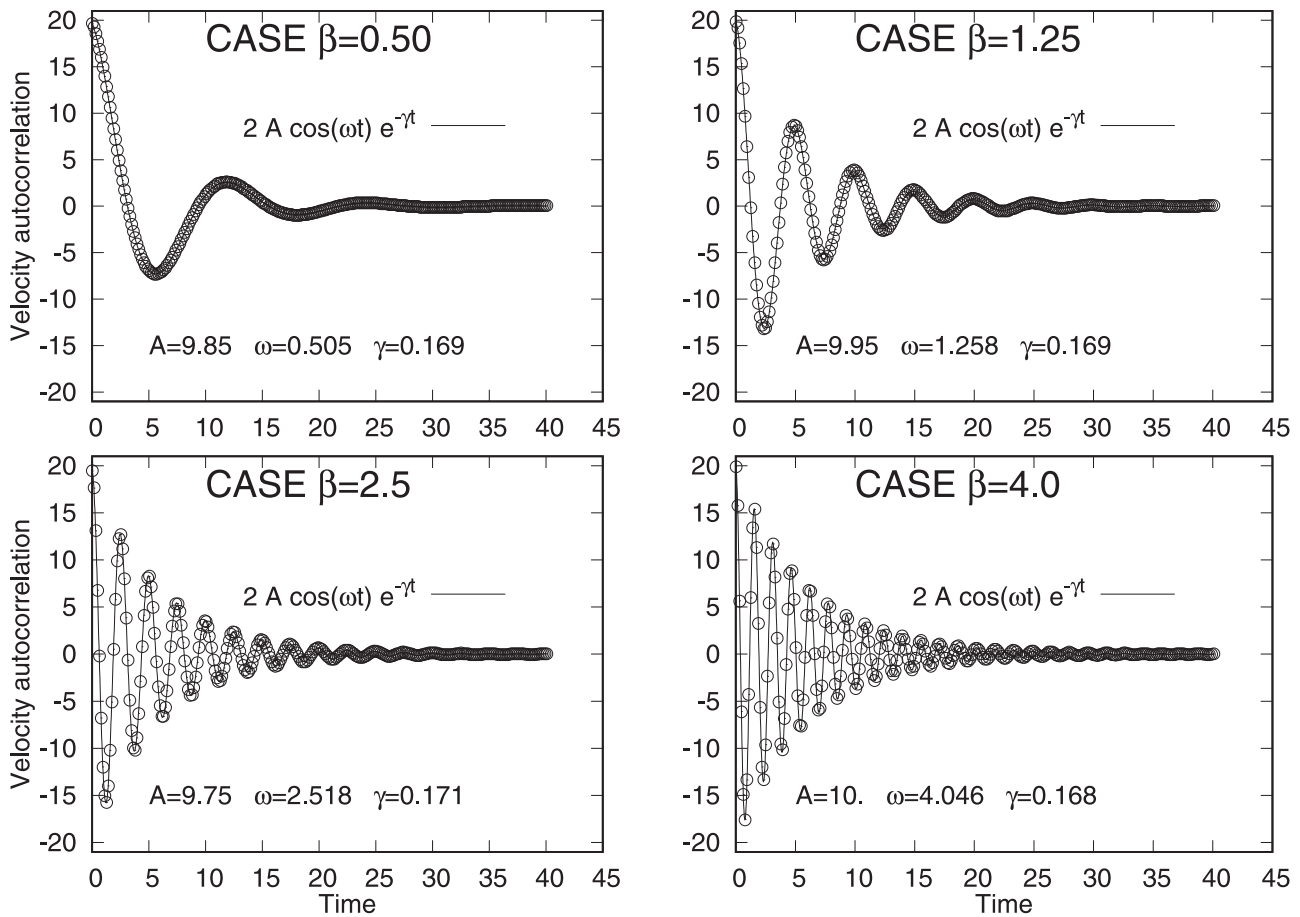


**FIG. 4.** Velocity autocorrelation  $(\vec{v}_\perp(t) \cdot \vec{v}_\perp(0))$ , as a function of time, for different values  $\beta = 0.5, \beta = 1.25, \beta = 2.5$ , and  $\beta = 5$ , of the magnetic field (circles), together with a best fit by a damped oscillation  $A \cos \omega t e^{-\gamma t}$  (solid line). The values of the parameter  $A, \gamma$ , and  $\omega$  are reported in each panel. The fit is very good either below and above  $\beta = 2$ . Notice that  $A, \gamma$  are essentially independent of  $\beta$ , while  $\omega$  agrees well with the cyclotron frequency  $\omega_c$ .

decay, and thus,  $f(t) = 2A e^{-\gamma t}$ , where  $\gamma$  is a parameter representing the inverse of the decorrelation time. Then, formula (9) gives exactly  $D_\perp = \frac{\gamma A}{\gamma^2 + \beta^2}$ .

In Fig. 4, the velocity autocorrelation is plotted as a function of time, for different values of  $\beta$ , either above and below the threshold  $\beta = 2$ . As one can check, the law (10) is nicely agreed. From the values reported in Table I, one finds that the parameters  $A$  and  $\gamma$  are quite independent of  $\beta$ , while  $\omega$  turns out to be very close to the cyclotron frequency  $\omega_c$  (equal to  $\beta$  in our units) as expected. Therefore, taking average values  $A = 9.9, \gamma = 0.168$ , and  $\omega = \omega_c$ , the values of the diffusion coefficient  $D_\perp$  obtained by numerical computations can be recovered from formula (9).

Now, a peculiar fact happens. In fact, while formula (10) appears to be in very good agreement with the velocity autocorrelation plots for all the values of  $\beta$  considered, the formula  $D_\perp = \frac{\gamma A}{\gamma^2 + \beta^2}$  is valid only below a threshold  $\beta_{cr} \simeq 2$ . This notwithstanding, if we compute the time integral numerically and inject it into formula (9), the resulting values of  $D_\perp$  agree very well with those found using

linear regression, as one can check from Table I comparing the values reported in the second and third column. Notice that, when computing the integral appearing formula (9), one has to truncate the integral to an upper limit  $t_{max}$  chosen carefully, i.e., not too large; otherwise, the numerical errors introduced in computing the autocorrelation  $(\vec{v}_\perp(t) \cdot \vec{v}_\perp(0))$  spoil the result.

A possible explanation of this transition when passing from a weakly magnetized to a strongly magnetized regime can be given in the spirit of Ref. 5, where it was surmised that at low  $\beta$ , the plasma is in a fully chaotic regime, but as  $\beta$  is increased, a transition to a partially ordered regime occurs.

It was shown in that paper how, in such a partially ordered regime, a perturbation theory could apply by adapting the Hamiltonian perturbation theory developed for system of interest in statistical mechanics (see, for example, Refs. 22–25) to the case of plasma. The idea is that, in the thermodynamical limit, one cannot control the adiabatic invariants along each individual trajectory (in the phase space), but it is instead possible to control their

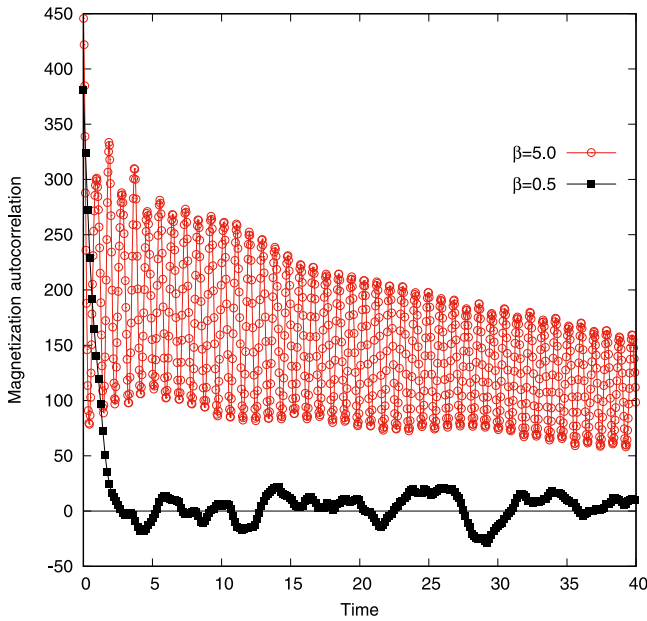


**FIG. 5.** Autocorrelation of the magnetization (along the magnetic field direction) as a function of time for two different values  $\beta = 0.5$  (square) and  $\beta = 5$  (circles) of the magnetic field. Notice that for a field below the threshold, the autocorrelation vanishes very fast, while, above the threshold, autocorrelation vanishes eventually on a totally different time scale.

autocorrelations with respect to an invariant measure, showing that they vanish exponentially slow in the perturbative parameter. Notice that, in virtue of the linear response theory, such autocorrelations correspond often to important physical observables.

In Ref. 5, it was considered the case of the component  $M$  of the magnetization along the magnetic field  $\vec{B}$ , defined (as usual) as

$$M \stackrel{\text{def}}{=} \frac{e}{2mc} \frac{1}{N} \sum_k (\vec{v}_k \times \vec{x}_k)_z. \quad (11)$$

Notice that the autocorrelation  $\mathcal{C}_M(t) \stackrel{\text{def}}{=} \langle M(t)M(0) \rangle$  is an important quantity because, according to the linear response theory, its Fourier transform  $\hat{\mathcal{C}}_M(\omega)$  gives the magnetic susceptibility  $\chi(\omega)$  at the frequency  $\omega$  (see, for example, Refs. 26 and 27 or Appendix B of Ref. 28).

In our case, the behavior of the autocorrelation is different below and above the threshold. This is shown in Fig. 5: for a low magnetic field, the autocorrelation relaxes to zero, while for a high magnetic field, it keeps oscillating and eventually vanishes on a totally different time scale. Therefore, the magnetization could be considered an adiabatic invariant of the system, thus implying that the dynamics remains partially correlated for a long time.

A similar mechanism could be at work also in the case of the velocity autocorrelation, even if from our plots, this is not as evident as in the case of the magnetization. In fact, a clue can be obtained by looking at the spectrum of the velocity autocorrelation, i.e., at their cosine Fourier transform, as shown in Fig. 6 (in a semilogarithmic

scale). Notice that  $D_\perp$  is simply half the value of the spectrum at  $\omega = 0$ .

For  $\beta = 0.5$ , the slope of the spectrum seems to vanish at  $\omega = 0$ . As the spectrum is an even function of the frequency, this is coherent with the behavior of a smooth function. On the contrary, for  $\beta = 5$ , the spectrum slope seems to remain (negative and) different from zero at  $\omega = 0$ . Now, it can be very easily shown that by denoting with  $\hat{f}(\omega)$  the Fourier cosine transform of the function  $f(t)$  then, for  $t \rightarrow +\infty$ , one has  $f(t) = \frac{2}{\pi} \frac{1}{t^2} \left( -\hat{f}(0) + o(1) \right)$  if all the derivatives of  $\hat{f}(\omega)$  up to the second one are integrable.<sup>29</sup> Therefore, it seems that in our data on the velocity autocorrelation, there is a small component that decays very slowly (i.e., as  $t^{-2}$ ) to zero. Nevertheless, such a component gives a very big contribution to the diffusion coefficient (more than double the one due to the exponentially decreasing part  $2A e^{-\gamma t} \cos \omega t$ ).

In any case, at the moment, it is not clear, for what reason, in a less chaotic regime, the diffusion coefficient apparently decreases, as a function of  $\beta$ , at a slower rate with respect to the fully chaotic regime.

#### IV. FINAL CONSIDERATIONS

In this work, we performed MD simulations of a magnetized electron gas, also called a one component plasma. We have shown that such a system shows a transition between two different regimes as the value of the parameter  $\beta$  is raised above a critical threshold of about 2.

The transition occurs both on a macroscopic level, with a change in the diffusive behavior, and on a microscopic level as well: when the parameter is raised, the system passes from a chaotic state to a partially ordered one. This is the main finding that we have pointed out, and is a rather new phenomenon, only remotely addressed in the literature up to now. As a matter of fact, a similar result, for what concerns the behavior of the diffusion coefficient, was published quite recently in Ref. 16. However, the authors tried to explain this phenomenon in the framework of the kinetic theory, looking at the behavior of the particles during the “collisions.” We refrain from this approach, and we try to discuss it according to the ergodic theory of a dynamical system using its standard tools. In particular, our aim is to understand if the dynamics is truly chaotic or not, and, in this latter case, what are the consequences for what concerns the macroscopic quantity characterizing the plasma.

As regards the direct consequences of our results on plasma physics, a strong objection may be raised on the dependence, we have not explored, of the results on the number of particles  $N$ . In particular, in Ref. 16, it was claimed that a few hundred particles are sufficient in the low  $\beta$  regime, but for high  $\beta$ , a huge number of particles (above  $10^6$ ) is needed. In particular, they show that the value of the diffusion coefficient slowly decreases as  $N$  is increased. However, it seems unlikely that those values would ever agree with the kinetic law  $D_\perp \propto \beta^{-2}$ , although a Bohm relation  $D_\perp \propto \beta^{-1}$  may finally show up in the high  $\beta$  regime, as in Ref. 9. Also, such a high value of  $N$  is going toward the real number of particles; therefore, at this point, even the use of periodic boundary conditions becomes questionable. Finally, possibly, the problem is that the diffusive regime is

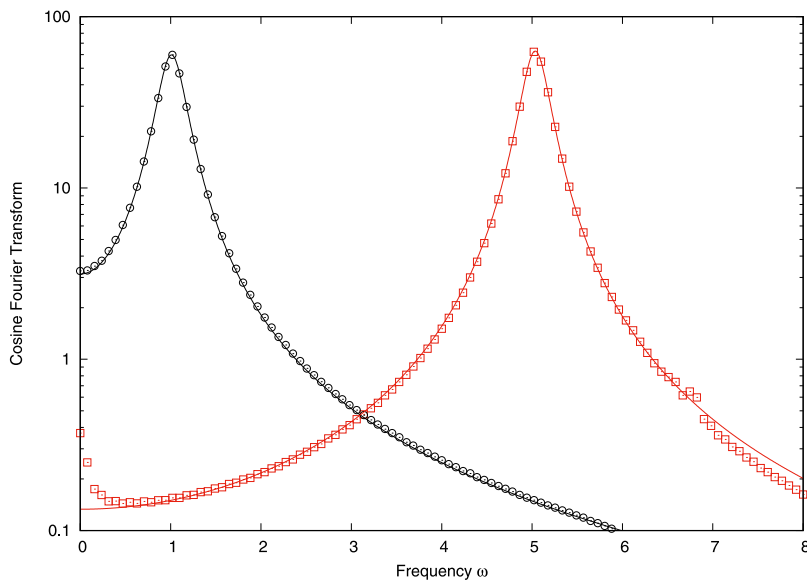


**FIG. 6.** Spectrum of the velocity as a function of  $\omega$  in a semilogarithmic scale for two different values of  $\beta = 0.5$  (circle) and  $\beta = 5$  (square). The continuous lines are the Fourier transform of the damped oscillation  $2Ae^{-\gamma t} \cos \omega t$ . For  $\beta = 1.0$ , the slope of the spectrum vanishes at  $\omega = 0$ ; for  $\beta = 5$ , the slope remains different from zero. This latter case hints at a decay of the velocity autocorrelation as  $1/t^2$  for  $t \rightarrow +\infty$  (see the text).

not normal so that the diffusion coefficient is not well defined. This problem is discussed at length in Ref. 1.

In any case, we think that there are much more fundamental questions to address about the portability of our results to real plasmas: above all, the absence of positive ions in our models. We hope to be able to address such a big issue in the (near) future.

## AUTHOR DECLARATIONS

### Conflict of Interest

The authors have no conflicts to disclose.

## DATA AVAILABILITY

The data that support the findings of this study are available from the corresponding author upon reasonable request.

## REFERENCES

- <sup>1</sup>R. Balescu, *Aspects of Anomalous Transport in Plasmas*, Series in Plasma Physics Vol. 18 (Taylor & Francis, 2005).
- <sup>2</sup>G. M. Zaslavsky, *Phys. Rep.* **371**, 461 (2002).
- <sup>3</sup>C. L. Longmire and M. N. Rosenbluth, *Phys. Rev.* **103**, 507 (1956).
- <sup>4</sup>A. Carati, F. Benfenati, A. Maiocchi, M. Zuin, and L. Galgani, *Chaos* **24**, 013118 (2014).
- <sup>5</sup>A. Carati, M. Zuin, A. Maiocchi, M. Marino, E. Martines, and L. Galgani, *Chaos* **22**, 033124 (2012).
- <sup>6</sup>D. F. Escande, *Plasma Phys. Control. Fusion* **58**, 113001 (2016).
- <sup>7</sup>G. G. Zimbardo, P. Veltri, and P. Pommois, *Phys. Rev. E* **61**, 1940 (2000).

<sup>8</sup>M. Allen and D. Tildesley, *Computer Simulation of Liquids* (Clarendon Press, Oxford, 1991).

<sup>9</sup>T. Ott and M. Bonitz, *Phys. Rev. Lett.* **107**, 135003 (2011).

<sup>10</sup>M. B. Isichenko, *Plasma Phys. Control. Fusion* **33**, 809 (1991).

<sup>11</sup>M. B. Isichenko, *Rev. Mod. Phys.* **64**, 961 (1992).

<sup>12</sup>J. Daligault, *Phys. Rev. Lett.* **108**, 225004 (2012).

<sup>13</sup>D. Saumon, C. E. Starrett, and J. Daligault, "Diffusion coefficients in white dwarfs," [arXiv:1410.7645](https://arxiv.org/abs/1410.7645) (2014).

<sup>14</sup>M. E. Caplan and I. F. Freeman, *Mon. Not. R. Astron. Soc.* **505**, 45 (2021).

<sup>15</sup>S. D. Baalrud and J. Daligault, *Phys. Rev. E* **96**, 043202 (2017).

<sup>16</sup>K. R. Vidal and S. D. Baalrud, *Phys. Plasmas* **28**, 042103 (2021).

<sup>17</sup>P. Gibbon and G. Sutmann, in *Quantum Simulations of Complex Many-Body Systems: From Theory to Algorithms*, NIC Series Vol. 10 (John von Neumann Institute for Computing, Jülich, 2002), pp. 467–506.

<sup>18</sup>E. Haire, C. Lubich, and G. Wanner, *Geometric Numerical Integration*, 2nd ed. (Springer, Berlin, 2009).

<sup>19</sup>J. Perram, H. Petersen, and S. Leeuw, *Mol. Phys.* **65**, 875 (1988).

<sup>20</sup>It is possible to conceive algorithms with an even slower asymptotic growth, but for the order of magnitude of  $N$  that we are considering, the Ewald summation formula works best.

<sup>21</sup>G. H. Wannier, *Statistical Physics*, rev. ed. (Dover Publications, New York, 2010).

<sup>22</sup>A. Carati, *J. Stat. Phys.* **128**, 1057 (2007).

<sup>23</sup>A. Carati and A. Maiocchi, *Commun. Math. Phys.* **314**, 129 (2012).

<sup>24</sup>A. Giorgilli, S. Paleari, and T. Penati, *Ann. Henri Poincaré* **16**, 897 (2015).

<sup>25</sup>W. De Roeck and F. Huvneers, *Pure Appl. Math.* **68**, 1532 (2015).

<sup>26</sup>R. Kubo, *J. Phys. Soc. Jpn.* **12**, 570 (1957).

<sup>27</sup>Y. Klimontovich, *Statistical Physics* (Taylor & Francis, New York, 1986).

<sup>28</sup>A. Carati, F. Benfenati, and L. Galgani, *Chaos* **21**, 023134 (2011).

<sup>29</sup>This can be inferred by the inverse transform formula  $f(t) = \frac{2}{\pi} \int_0^{+\infty} \hat{f}(\omega) \cos \omega t d\omega$  by integrating two times by part and using the Riemann–Lebesgue lemma on the remainder.